

Provided for non-commercial research and education use.
Not for reproduction, distribution or commercial use.



This article appeared in a journal published by Elsevier. The attached copy is furnished to the author for internal non-commercial research and education use, including for instruction at the authors institution and sharing with colleagues.

Other uses, including reproduction and distribution, or selling or licensing copies, or posting to personal, institutional or third party websites are prohibited.

In most cases authors are permitted to post their version of the article (e.g. in Word or Tex form) to their personal website or institutional repository. Authors requiring further information regarding Elsevier's archiving and manuscript policies are encouraged to visit:

<http://www.elsevier.com/copyright>



Contents lists available at ScienceDirect

Journal of Theoretical Biology

journal homepage: www.elsevier.com/locate/jtbi

The effects of density-dependent dispersal on the spatiotemporal dynamics of cyclic populations

Matthew J. Smith^{a,b,c,*}, Jonathan A. Sherratt^b, Xavier Lambin^c

^a Computational Ecology and Environmental Science Group, Microsoft Research Limited, Cambridge CB3 0FB, UK

^b Department of Mathematics and the Maxwell Institute for Mathematical Sciences, Heriot-Watt University, Edinburgh EH14 4AS, UK

^c Institute of Biological and Environmental Sciences, Zoology Building, University of Aberdeen, Tillydrone Avenue, Aberdeen AB24 2TZ, UK

ARTICLE INFO

Article history:

Received 14 November 2007

Received in revised form

28 May 2008

Accepted 28 May 2008

Available online 1 June 2008

Keywords:

AUTO

Larch budmoth

Lambda-omega

Landscape obstacle

Numerical continuation

Predator-prey

Invasion

Wave train

ABSTRACT

Density-dependent dispersal occurs throughout the animal kingdom, and has been shown to occur in some taxa whose populations exhibit multi-year population cycles. However, the importance of density-dependent dispersal for the spatiotemporal dynamics of cyclic populations is unknown. We investigated the potential effects of density-dependent dispersal on the properties of periodic travelling waves predicted by two coupled reaction–diffusion models: a commonly used predator–prey model, and a general model of cyclic trophic interactions. We compared the effects of varying the gradient of both positive and negative density-dependent dispersal rates, to varying the ratio of the (constant) dispersal rates of the two interacting populations. Our comparison focussed on the possible range of wave properties, and on the waves generated by landscape obstacles and invasions. In all scenarios that we studied, varying the gradient of density-dependent dispersal has small quantitative effects on the travelling wave properties, relative to the effects of varying the ratio of the diffusion coefficients.

© 2008 Elsevier Ltd. All rights reserved.

1. Introduction

Periodic travelling waves of abundance have been recorded in ecological systems exhibiting cyclic multi-year dynamics, for a wide range of taxonomic groups (Bjørnstad et al., 2002; Giraudoux et al., 1997; Lambin et al., 1998; Mackinnon et al., 2001; Moss et al., 2000; Murray et al., 1986; Ranta and Kaitala, 1997; Russell et al., 2005; Tenow et al., 2007; Sherratt and Smith, 2008). A commonly used method for mathematically modelling such systems is to start with a non-spatial model of a cyclic ecological system, and then to add random dispersal to each of the component equations. This assumes that individuals in these populations move, or diffuse, throughout their environment in random directions at a specified rate; obviously a major simplification of dispersal in nature. Such “reaction–diffusion” models predict a variety of spatiotemporal patterns that have been observed in ecological systems: spatially homogeneous oscillations, travelling waves (see Fig. 1 for example), invasive fronts, and irregular spatiotemporal behaviour (Kopell and

Howard, 1973; Murray, 2003; Petrovskii and Malchow, 1999). This has led to the theory that the periodic travelling waves observed in ecological systems may be caused by dispersal acting on cyclic populations.

Travelling waves in ecological systems are commonly characterised by their wavelength (e.g. in km), amplitude (i.e. the range of population density), speed (km yr^{-1}) or time period (yr). Note that by “time period” we are referring to the temporal period of oscillation that would be recorded at a fixed position in space; this would typically be of 3–10 yr in populations that exhibit multi-year cycles (Berryman, 2002). Mathematical analysis of reaction–diffusion models shows that, for a given model with a specific set of parameters, there is a spectrum of possible wave characteristics (Kopell and Howard, 1973; Murray, 2003). Fig. 1(a) illustrates this “wave family” for a commonly used predator–prey model with a given set of parameters, plotted as wavelength against time period. In this case, the wave family shown has a minimum wavelength, with all wavelengths above this being possible. Infinite wavelengths correspond to spatially homogeneous oscillations: these are simply the cyclic solutions (limit cycle) of the non-spatial predator–prey model.

Any reaction–diffusion model can be simulated with a variety of different initial conditions, spatial configurations, and boundary conditions, to represent different ecological scenarios. Such conditions determine whether periodic travelling waves emerge

* Corresponding author at: Computational Ecology and Environmental Science Group, Microsoft Research Limited, Cambridge CB3 0FB, UK. Tel.: +44 1223479784.

E-mail addresses: Matthew.Smith@microsoft.com (M.J. Smith), j.a.sherratt@ma.hw.ac.uk (J.A. Sherratt), x.lambin@abdn.ac.uk (X. Lambin).

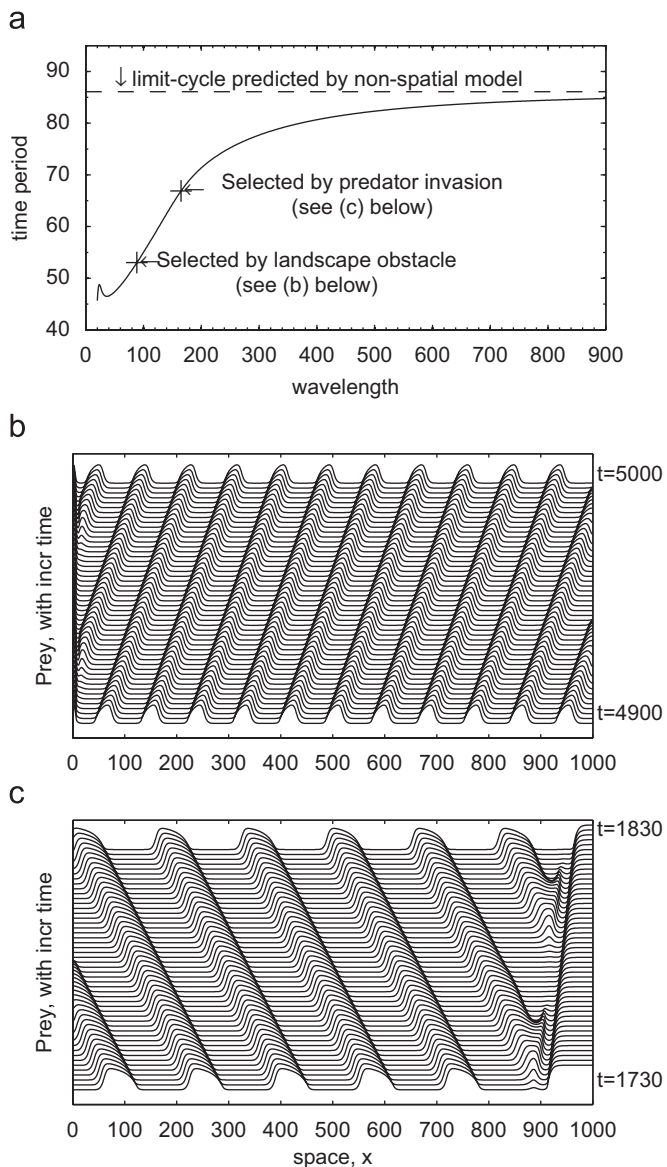


Fig. 1. (a) An example of a travelling wave family predicted by a predator–prey reaction–diffusion model (Eqs. (1a) and (1b) with reaction kinetics (2) and density-dependent dispersal function (4)). The parameter values are $\sigma = 0.15$, $\mu = 0.05$, and $\kappa = 0.2$, $D_{u,max} = 10^{0.5}$, $D_{u,min} = 10^{-0.5}$ (implying $D_v = 1$) and $m = -100$ (these parameter values are defined in the text). (b) and (c) show periodic travelling waves arising from two different selection mechanisms in simulations of the same model as in (a) and, hence, they are selected from the same wave family; marked with labelled crosses in (a). A landscape obstacle is assumed in (b), with $(u, v) = (0, 0)$ at the left boundary (simulating an inhospitable habitat at $x < 0$) and $du/dx = dv/dx = 0$ at the right boundary. This simulation started with random initial predator and prey densities. (c) Simulates predators invading a prey population, with $du/dx = dv/dx = 0$ assumed at both boundaries. This simulation started with the prey-only steady state, $(u, v) = (1, 0)$, throughout the domain except the left boundary, which started with $(u, v) = (1, 1)$. Note that the invasion front (where prey density sharply declines from $(u = 1)$) has travelled to the right of the domain in this scenario. Animations of the dynamics in this figure, and other figures in this paper, can be generated and explored using the custom made software tool that is downloadable from <http://research.microsoft.com/ero/biosciences/software.aspx>.

in simulations, and the properties of those waves if they do emerge. From an ecological perspective, the most commonly studied environmental scenarios for which periodic travelling waves have been observed are environments with landscape obstacles (Auchmuty and Nicolis, 1976; Sherratt et al., 2003) and invasions (Ashwin et al., 2002; Ermentrout et al., 1997; Garvie,

2007; Pearce et al., 2006; Petrovskii and Malchow, 1999; Sherratt et al., 1997). These two “wave selection” mechanisms give rise to different members of the wave family (Sherratt, 2001, 2003); this is illustrated in Figs. 1(b) and (c).

The assumption that an individual's dispersal is simply a random diffusive process is obviously a crude simplification. In reality, dispersal is not simply a rate of movement, but is a complex process determining the movement of individuals from one area to another. Dispersal can be conveniently broken into three stages: emigration, movement between areas, and immigration. An individual's propensity to emigrate from, and immigrate into an area, and its behaviour whilst dispersing, can depend on a wide variety of ecological factors (Ims and Hjermann, 2001; Sutherland et al., 2002), of which the local density of individuals is one that has been shown to affect the dispersal behaviour of a wide range of animal taxa (Bowler and Benton, 2005; Denno and Peterson, 1995; Matthysen, 2005).

In general, there is evidence that dispersal rates in all three stages of the dispersal process can vary positively, negatively, or not at all with population density. For example, many mammal, bird and insect taxa exhibit positive density-dependent emigration (Denno and Peterson, 1995; Matthysen, 2005). This may arise for a variety of reasons such as competition for food or mates, and inbreeding avoidance (Bowler and Benton, 2005; Ims and Hjermann, 2001; Lambin et al., 2001; Sutherland et al., 2002). In contrast, negative density-dependent emigration rates may be a general characteristic of territorial species (Lambin et al., 2001; Matthysen, 2005). This could arise because increasing population density could lead to an increase in the likelihood of aggressive encounters, which in turn could result in reduced movement rates (Lambin et al., 2001; Matthysen, 2005). For immigration rates, knowledge is lacking for most species, although it has been found to be negatively density dependent in some studies (Kuussaari et al., 1996; Rouquette and Thompson, 2007; Smith and Batzli, 2006).

For cyclic populations, there is little empirical data on dispersal rates and dispersal propensity. There is widespread evidence that trophic interactions such as predator–prey, host–parasite, and vegetation–grazer are important in the dynamics of cyclic populations (Berryman, 2002), yet the dispersal properties of the interacting components in these interactions are poorly understood. It has been generally suggested that long distance dispersal by certain species may generate spatial synchrony in the cycles at the landscape scale, with examples being the nomadic predators in Fennoscandia (Ydenberg, 1987), the canadian lynx (Schwartz et al., 2002) and the spruce budworm (Royama et al., 2005). Density-dependence in dispersal is much less well understood for cyclic populations. However, in several studies of cyclic rodent species it has been shown that emigration rates and dispersal distances are negative-density dependent (reviewed by Matthysen (2005)).

Theoretical studies have explored the significance of density-dependent dispersal for the dynamics of single populations (Lutscher, 2008), metapopulations (Best et al., 2007; Saether et al., 1999), trophic interactions (Huu et al., 2008), the stability of local population dynamics (Amarasekare, 1998; Johst and Brandl, 1997), and the degree of synchrony between populations connected by dispersal (Ims and Andreassen, 2005; Ylikarjula et al., 2000). In most cases, these have shown that density-dependent dispersal can affect the dynamics predicted by such models, although Ylikarjula et al. (2000) found that the effects of density-dependent dispersal on population synchrony was largely dependent on other details included in the model. Similar studies for cyclic populations are lacking.

In this paper we investigate the effects of density-dependent dispersal on the properties of periodic travelling waves in cyclic

populations. We study a reaction–diffusion model of the population dynamics of two interacting populations, of the form

$$\frac{\partial u}{\partial t} = \overbrace{\frac{\partial}{\partial x} \left(D_u(u) \frac{\partial u}{\partial x} \right)}^{\text{Dens.dep. dispersal}} + \overbrace{f(u, v)}^{\text{Birth and death}}, \quad (1a)$$

$$\frac{\partial v}{\partial t} = \underbrace{D_v \frac{\partial^2 v}{\partial x^2}}_{\text{Dispersal}} + \underbrace{g(u, v)}_{\text{Birth and death}}, \quad (1b)$$

where t is time, x is space, u and v are the component population densities, and D_u, D_v are the dispersal rates. We assume that one population (v) disperses randomly at a constant rate and the other (u) disperses at a potentially density-dependent rate. In this study, therefore, dispersal is simply an individual's rate of movement in a uniform habitat. We do not model emigration or immigration as independent processes, nor do we model patchy environments. The use of diffusion as a model for biological dispersal was recently reviewed by Codling et al. (2008). We also assume that, in the absence of dispersal, Eqs. (1a) and (1b) predict population cycles.

Current mathematical theory does not enable us to determine analytically the precise member of the wave family selected by wave selection mechanisms, except in a few special cases (Drover and Ermentrout, 2003; Ermentrout et al., 1997; Sherratt, 1994, 2003). In view of this, we addressed our question using two basic approaches. We first studied the effects of density-dependent dispersal on the shape of the whole travelling wave family (such as shown in Fig. 1(a)), since any wave must be selected from this. This is important because, for example, the incorporation of density-dependent dispersal could cause waves of a given time period, for example 9 yr in the cyclic larch budmoth populations in Switzerland (Turchin, 2003), to have much shorter or longer wavelengths than is the case for density independent dispersal. Such differences may determine whether periodic travelling waves can be detected in the field; for example wavelengths comparable with or greater than the size of the area being sampled would be detected as environmentally homogeneous oscillations. Secondly, we studied waves that arise in simulations of our reaction–diffusion model, as a result of two different wave selection mechanisms: a landscape obstacle and predator–invasion (Fig. 1(b, c)).

Our key variable of interest will be the gradient with which dispersal rate changes as a function of population density. To obtain a measure of the relative effects of the gradient of density-dependent dispersal, we compare our results to the effects of assuming constant dispersal rates and varying their ratio. This ratio is likely to vary considerably among different ecological interactions predicting multi-year cycles. If, for example, we assume that Eqs. (1a) and (1b) model consumer–resource interactions (e.g. predator–prey, host–parasite), where u is the resource (e.g. prey) and v is the consumer (e.g. predator), then the dispersal ratio D_u/D_v could be quite different depending on the interaction being modelled. For mammalian predator–prey interactions, for example, terrestrial predators are likely to move at least one or two orders of magnitude faster than their prey (Brandt and Lambin, 2007), corresponding to dispersal ratios (D_u/D_v) of much less than 1. One extreme is a plant–herbivore interaction (Massey et al., 2008), for which the dispersal ratio is zero. Dispersal rates are typically more similar to each other in aquatic systems (Hauzy et al., 2007), and in host–parasite interactions (Moss et al., 2000). An example of a cyclic population in which the resource (prey) moves faster than the consumer (predator) occurs in the larch budmoth–parasitoid interaction in the European Alps (Baltensweiler et al., 1977; Peltonen et al.,

2002); here the dispersal ratio is greater than 1. A mathematical investigation into the effects of varying the dispersal ratio (D_u/D_v) on periodic travelling wave properties was recently conducted by Smith and Sherratt (2007), who found that this ratio can have considerable effects on the travelling wave properties. These provide a natural comparison for our study of the effects of varying the gradient of density-dependent dispersal.

2. Methods

2.1. The specific population models

The functions f and g in Eqs. (1a) and (1b) are commonly referred to as the ‘reaction kinetics’. These could be taken from any two-taxon continuous time population model that predicts population cycles (see Turchin, 2003 for several examples). We consider two commonly used forms of these functions. The first is a predator–prey model (Rosenzweig and MacArthur, 1963; Turchin, 2003), with

$$f(u, v) = u(1 - u) - \frac{uv}{u + \kappa}, \quad (2a)$$

$$g(u, v) = \frac{\sigma uv}{u + \kappa} - \mu v, \quad (2b)$$

where u and v are the densities of prey and predators, respectively, μ is the predator death rate, σ is the prey to predator conversion rate, and κ is the half-saturation constant in the rate of prey consumption by predators. These equations have been non-dimensionalised so that their parameters have no units; see Appendix A for the equations in dimensional form. In these rescaled equations, prey population density can vary between 0 and 1. Throughout this study we fix $\sigma = 0.15$, $\mu = 0.05$, and $\kappa = 0.2$. These parameter values were not derived from any specific ecological system. With these kinetics and parameter values, Eqs. (1a) and (1b) have three unstable spatially uniform steady states: one is where both populations are zero ($(u, v) = (0, 0)$), one is prey-only ($(u, v) = (1, 0)$), and one is predator–prey coexistence ($(u, v) = (u_s, v_s) = (0.1, 0.27)$). For these equations, we assume that it is the prey population that could potentially move at a density-dependent rate. This assumption is most relevant to scenarios in which predators are prey-limited, so that their populations never reach densities where crowding would affect their dispersal behaviour. This assumption is also commonly made to justify the lack of density-dependence in the rate of change of the predator population (Turchin, 2003).

The second set of reaction kinetics we consider are

$$f(u, v) = (1 - r^2)u - (w_0 - w_1 r^2)v, \quad (3a)$$

$$g(u, v) = (1 - r^2)v + (w_0 - w_1 r^2)u, \quad (3b)$$

where $r = (u^2 + v^2)^{1/2}$, $w_0 = 1.5$ and $w_1 = 0.5$. Eqs. (1a) and (1b) with these kinetics are commonly referred to as being of ‘lambda–omega’ type (Kopell and Howard, 1973). We chose the lambda–omega equations because they are the most general representation of two-taxon interactions that generate population cycles. In fact, they predict the dynamics of all systems modelled by Eqs. (1a) and (1b) when the population cycles are of low amplitude relative to their mean; mathematically, the kinetics are the normal form of a standard Hopf bifurcation (Hagan, 1982). The predictions from these equations are therefore a ‘control’ with which to compare the results of scenario-specific equations, such as the predator–prey equations studied here. The lambda–omega equations have an unstable spatially uniform steady state at $(u, v) = (u_s, v_s) = (0, 0)$, and when the dispersal rates are

constant and equal they predict identical (but out of phase) spatial and temporal dynamics for both population components.

2.2. The density-dependent dispersal function

We use a logistic form for the shape of the density-dependent dispersal function, $D_u(u)$:

$$D_u(u) = 10^{\left(\frac{\log_{10}(D_{u,max}) - \log_{10}(D_{u,min})}{1 + \exp(m(u_s - u))} + \log_{10}(D_{u,min}) \right)} \quad (4)$$

where $D_{u,max}$ and $D_{u,min}$ are the maximum and minimum dispersal rates, respectively. We assume that the population density at the inflexion point of the logistic relationship is u_s , the unstable equilibrium value of prey in the presence of predators ($u_s = 0.1$) in the case of reaction kinetics (2), or simply the unstable equilibrium value of u ($u_s = 0$) in Eqs. (3a) and (3b). Fig. 2 gives plots of Eq. (4) for the two different sets of reaction kinetics and for different values of m . Note that $m = 0$ corresponds to constant dispersal rates, $m > 0$ corresponds to positive density-dependent dispersal, and $m < 0$ corresponds to negative density-dependent dispersal. Note also that at highly positive or negative values of m , the density-dependent dispersal relationship becomes similar to a step function.

2.3. Parameter ranges

In this study, we are interested in the effects of increasing or decreasing the gradient of density-dependence in the dispersal rate (parameter m in Eq. (4)) from $m = 0$ (constant dispersal rate), on the predictions of Eqs. (1a) and (1b). We studied m in the range shown in Fig. 2 ($-100 \leq m \leq 100$), whilst fixing $D_u(u_s) = D_v = 1$, $D_{u,max} = 10^{(0.5)}$, and $D_{u,min} = 10^{(-0.5)}$. This means that the dispersal rate of u can potentially fluctuate above and below that of v . We made this decision for parsimony but we have also performed investigations in which D_u is always less than, or always greater than, D_v , as is likely to be the case in certain ecological systems, and found the same general results as those reported here. Note that the ratio $D_u(u)/D_v$ cannot vary by more than one order of magnitude. This represents extreme variation in the dispersal rates as a function of density, based on the literature cited in Bowler and Benton (2005), Denno and Peterson (1995) and Matthysen (2005).

To obtain a relative measure of the effects of varying m , we compare our results to the effects of assuming constant dispersal rates ($m = 0$) and varying their ratio, $\alpha = D_u(u_s)/D_v$ between 0.01

and 100. For the predator–prey equations, this would therefore translate as the prey moving a hundred times slower or faster than the predator, respectively. Whilst more extreme ratios may exist for some ecological systems, as detailed in the Introduction, we restricted ourselves to this range as it captures the general effects of varying α in our chosen equations, and is certainly sufficient to enable an effective comparison between variations in α and m . Note that for the lambda–omega kinetics, since the equations are symmetric about $u = 0$ and there are no differences in the dynamics of u and v , any effects of varying m or α will be symmetrical about $m = 0$ or $\alpha = 1$, respectively. These parameter choices mean that we are comparing variation of $D_u(u)/D_v$ by up to one order of magnitude (centred on $D_u(u_s)/D_v = 1$) with variation in $\alpha = D_u(u_s)/D_v$ of four orders of magnitude (when $m = 0$). We made this choice in order to focus on biologically plausible parameter ranges.

2.4. Numerical analysis of travelling wave families, and spatial simulations

We used the software package AUTO (Doedel, 1981) to analyse the travelling wave families predicted by Eqs. (1a) and (1b) for our different reaction kinetics and parameter ranges. One of the specific purposes of this software is to analyse families of periodic solutions to ordinary differential equations, into which Eqs. (1a) and (1b) can be converted. The methodology we used is standard and we refer the reader to Appendix B for more details of this analysis.

To conduct the spatial simulations of Eqs. (1a) and (1b), we assume one-dimensional space throughout, and use standard numerical techniques to solve the equations. The important differences between the scenarios are in the initial and boundary conditions.

In the landscape obstacle scenario we started with random initial values of u and v , drawn from a uniform distribution between 1 and 0. For each simulation, we fixed $(u, v) = (0, 0)$ at the left boundary and $du/dx = dv/dx = 0$ at the right boundary. This “pins” the population densities to zero at the left boundary, simulating an uninhabitable obstacle in the environment or a habitat boundary with a hostile environment (Cantrell et al., 1998), as illustrated in Fig. 1(b).

For the predator invasion scenario, it only makes sense to use the predator–prey reaction kinetics (2) as there is no analogue of the prey-only state in the lambda–omega equations. In this scenario we started with the prey-only steady state, $(u, v) = (1, 0)$,

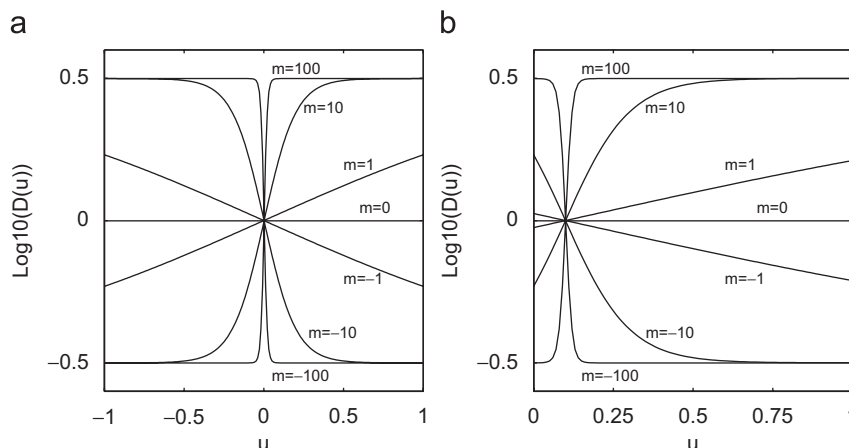


Fig. 2. The shapes of the relationship between population density, u , and the diffusion coefficient, $D_u(u)$ (Eq. (4)), for (a) the lambda–omega and (b) predator–prey reaction kinetics (Eqs. (3a), (3b), (2a) and (2b), respectively) and for different values of m , with $D_u(u_s) = 1$, $D_{u,max} = 10^{(0.5)}$, and $D_{u,min} = 10^{(-0.5)}$. Note that D_u varies on a log₁₀ scale. Positive and negative values of m correspond to positive and negative density-dependent dispersal, respectively.

throughout the domain except at the left boundary, which started with $(u, v) = (1, 1)$. We assumed $du/dx = dv/dx = 0$ at both boundaries. These conditions result in an invasion by the predator population into the (unstable) prey-only steady state. This can result in periodic travelling waves behind the invasion front, as illustrated in Fig. 1(c). Animations of the numerical dynamics illustrated in this paper can be generated and explored using the custom made software tool that is downloadable from <http://research.microsoft.com/ero/biosciences/software.aspx>.

3. Results

Throughout this section we will focus on the wave properties of wavelength and time period as these are typically the easiest solution measures to obtain from empirical data. We rescaled these quantities to aid comparison between the results, and with other systems. We set the minimum predicted wavelength, in the absence of density-dependent dispersal and when the dispersal rates are equal, to one, and scaled all other measured wavelengths relative to this. We also set the time period predicted by the non-spatial models (or spatially homogeneous oscillations) equal to one and scaled all measured time periods relative to this.

Fig. 3 contrasts the effects of varying the gradient of density-dependent dispersal (m) and the ratio of the constant dispersal rates (α), on the shape of the family of travelling wave solutions.

The simplest case to interpret is when gradient of density-dependent dispersal (m) is varied in the lambda-omega scenario (Fig. 3(a)). Here the wave families appear very similar for all values of m . The range of possible time periods for all three wave families varies from a maximum of one, corresponding to the limit cycle of the non-spatial model, down to about 65% of the limit cycle value. So, for example, if the unscaled non-spatial model predicted 10-yr cycles, then the spatial model could predict cycle periods down to 6.5 yr.

In comparison to varying the gradient of density-dependent dispersal in Eqs. (1a) and (1b) with the lambda-omega kinetics (3), varying the ratio of the diffusion coefficients (α) has a larger effect (Fig. 3(b)). Generally, varying α alters the point at which the wave family starts, and the range of possible time periods. When $\alpha = 100$ (with $m = 0$), for example, the minimum time period is about 88% that which would be predicted by the non-spatial equations, rather than about 65% when $\alpha = 1$. As a further example, the wavelength associated with a time period of 0.95 when $\alpha = 100$ is double that when $\alpha = 1$ (wavelength = 6 versus wavelength = 3, respectively).

When the underlying kinetics are the predator-prey equations, we observe larger effects of varying both the gradient of density-dependent dispersal (m) (Fig. 3(c)) and the ratio of the dispersal rates (α) (Fig. 3(d)), than in the lambda-omega equations. In general, the range of possible time periods for the predator-prey equations is larger than in the lambda-omega equations, with the

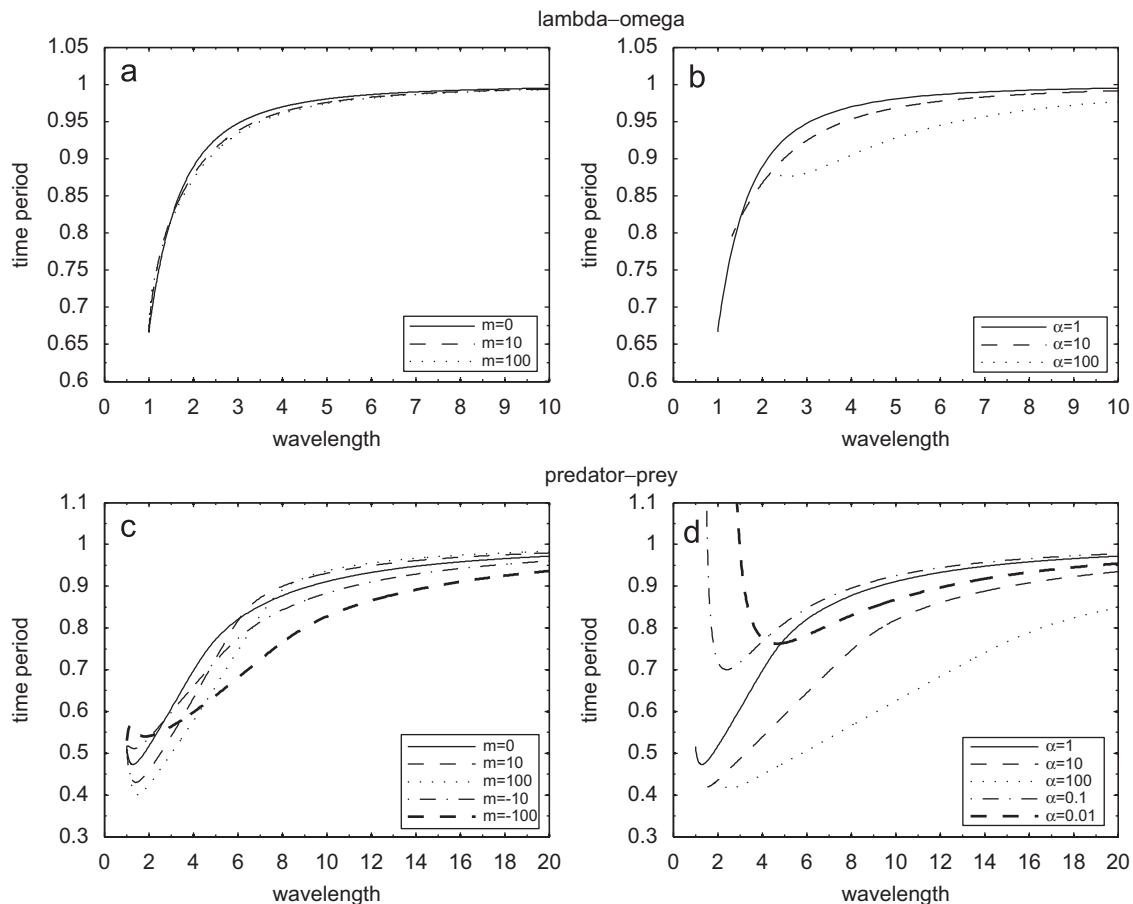


Fig. 3. Comparison of varying the gradient of density-dependent dispersal m , between -100 (strong negative density-dependence) and 100 (strong positive density-dependence) with varying the ratio of constant diffusion coefficients $\alpha = D(u_s)/D_v$ ($m = 0$) between 0.01 and 100 (log scale), on the shape of the travelling wave family predicted by Eqs. (1a) and (1b). (a) and (b) have lambda-omega kinetics (3) with $\omega_0 = 1.5$ and $\omega_1 = 0.5$. (c) and (d) have predator-prey kinetics (2) with $\sigma = 0.15$, $\mu = 0.05$, and $\kappa = 0.2$. $\alpha = 1$ in (a) and (c). $m = 0$ in (b) and (d). Dispersal parameter values are $D_{u,max} = 10^{0.5}$ and $D_{u,min} = 10^{-0.5}$, implying that $D_v = 1$. To aid interpretation we have rescaled both wavelength and time period, which simply relabelled the axes. We divided the time period by the time period predicted by the non-spatial models (corresponding to infinite dispersal rates in Eqs. (1a) and (1b)), and we divided the wavelength by that at the origin of the wave family when $m = 0$ and $\alpha = 1$.

minimum time period sometimes being less than 50% that of the non-spatial model. Increasing m above zero (positive density-dependence) alters both the minimum time period of the wave family and the time periods associated with given wavelengths. Therefore, for a given cyclic predator–prey system exhibiting periodic travelling waves, the measured period of oscillation could depend on the degree of density-dependent dispersal in the prey population. However, the effects of varying the gradient of density-dependent dispersal are small compared to the effects of varying α (Fig. 3(d)). For example, with no density-dependent dispersal ($m = 0$), and equal dispersal rates ($\alpha = 1$), a time period of 0.8 corresponds to a wavelength of almost 6. With strong negative density-dependent dispersal ($m = -100$) and equal dispersal rates the same time period corresponds to a wavelength of around 9, a 50% increase (Fig. 3(c)). In contrast, with no density-dependent dispersal and $\alpha = 100$ such a time period corresponds to a wavelength of about 17, a 183% increase (Fig. 3(d)). The general result from these analyses is that the gradient of density-dependent dispersal (m) does affect the travelling wave families, but that these effects appear to be small compared to the effects of assuming constant dispersal rates and varying their ratio (α).

Fig. 4 contrasts the effects of varying the gradient of density-dependent dispersal (m) and the ratio of the diffusion coefficients (α), on the wavelengths of waves picked out in simulations of Eqs. (1a) and (1b), for our two wave generation mechanisms.

To aid in the interpretation of the data, we have added lines corresponding to the minimum wavelength of the wave family (thick lines), and the wavelengths of waves of fixed time period (thin lines). These lines present information already given in Fig. 3, but in Fig. 4 they are shown for continuously varying m or α .

Again we observe in Fig. 4 that the effects of the gradient of density-dependent dispersal (m) are less than the effects of varying the ratio of the dispersal rates (α). The first thing to notice for the lambda-omega scenarios is that all of the waves selected by landscape obstacles (indicated by filled circles) have time periods that are close to that of the limit cycle of the non-spatial model (as indicated by the contour lines in Fig. 4(a, b)). In contrast, there is more variation in the wavelengths of the selected waves (Fig. 4(a, b)). Therefore, if these equations modelled two field systems that differed in the ratio of their dispersal rates (α) or the degree of density-dependent dispersal (m) only, then differences in the dynamics would be more apparent in the spatial data than from non-spatial time series. The wavelengths of waves picked out by landscape obstacles are smallest (wavelength = 4) when there is no density-dependent dispersal ($m = 0$) and the dispersal rates are equal ($\alpha = 1$). Increasing or decreasing m increases the wavelength but this variation visibly saturates, at around $|m| = 20$, and at a wavelength of about 7 (a 75% increase). In contrast, increasing or decreasing α from 1 causes the predicted wavelength to

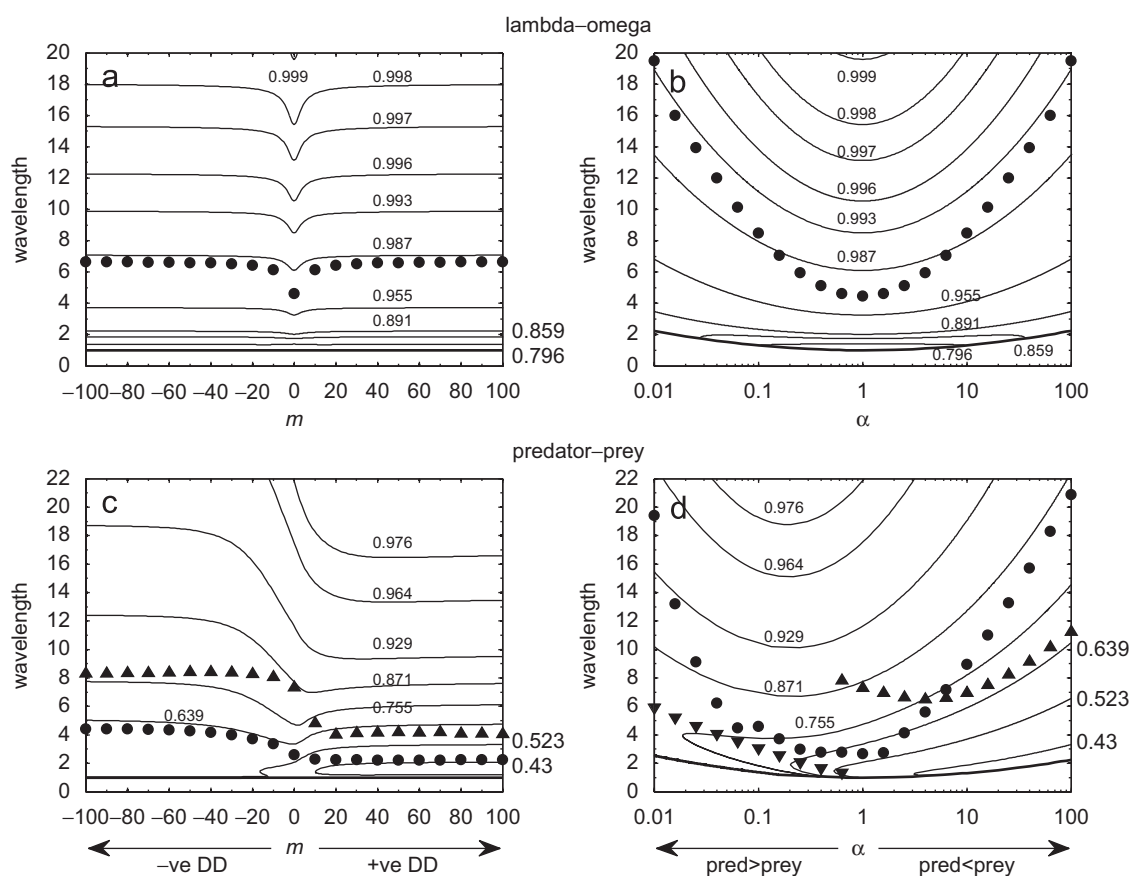


Fig. 4. Comparison of varying the gradient of density-dependent dispersal m , between -100 (strong negative density-dependence) and 100 (strong positive density-dependence) with varying the ratio of constant diffusion coefficients $\alpha = D_u/D_v$ ($m = 0$) between 0.01 and 100 , on the wavelengths of periodic travelling waves (symbols) picked out by simulations of Eqs. (1a) and (1b). Note that α determines D_u and D_v , because our non-dimensionalization implies that $D_u D_v = 1$. (a) and (b) have lambda-omega kinetics (3) and (c) and (d) have predator-prey kinetics (2). $\alpha = 1$ in (a) and (c). $m = 0$ in (b) and (d). Parameter values are the same as those detailed in the legend to Fig. 3. Filled circles denote the wavelengths of periodic travelling waves resulting from simulations with a landscape obstacle. In all of these cases the waves travel away from the obstacle edge (as demonstrated in Fig. 1(b)). Triangles denote the wavelengths of periodic travelling waves resulting from predator invasion into a prey population. Upwards pointing triangles denote waves moving to the left, in the opposite direction to the invasion front, and downwards pointing triangles denote waves moving to the right. Superimposed on the graphs are contour lines of fixed time period (thin lines), and the minimum wavelength (thick lines) from the analysis of the travelling wave families. To aid interpretation we have rescaled both wavelength and time period, which simply relabelled the axes, as detailed in the legend to Fig. 3.

continually increase, with the highest recorded wavelengths (wavelength = 20, a 400% increase) occurring at the smallest and largest values of α ($|\alpha| = 100$).

In the predator–prey equations, the wavelength and time period of waves picked out by simulations vary more than in the lambda–omega equations (circles and triangles in Figs. 4(c) and (d)). Furthermore, for some parameter values, waves are picked out with time periods that are considerably less than those predicted by the non-spatial model (some less than 50%, as indicated by the time period contour lines). As for the lambda–omega equations, we observe that for both mechanisms, as the gradient of density-dependent dispersal (m) is varied from zero, the effects on the properties of the selected waves visibly saturates at around $|m| \approx 20$. Again for both selection mechanisms reducing m from zero increases the wavelength of selected waves from around 3 and 7 at $m = 0$, to around 4 and 8 at $m = -100$, in the landscape obstacle (circles) and predator invasion (triangles) scenarios, respectively. Increasing m from zero has the opposite effect; with wavelength decreasing to 2 and 4 at $m = 100$. Note that waves selected by predator invasion (triangles) always produce higher wavelength and time period waves than those produced by zero-boundary conditions (circles; Fig. 4(c, d)). This illustrates that variation in travelling wave properties may be due to a different wave selection mechanism, as well as differences in the ratio and density-dependence of the dispersal rates.

As in the lambda–omega equations, the wavelengths of waves selected by the landscape obstacle in the predator–prey equations increase with variation in the ratio of the dispersal rates (α) away from one (other than a small dip near $\alpha = 0.1$; circles in Fig. 4(d)). In this case, however, variation in wavelength is accompanied by appreciable changes in the predicted time period. For example, when there are equal dispersal rates ($\alpha = 1$) the landscape obstacle selects a wave with a wavelength of just over 2, with a time period of 60% that of the non-spatial model, whereas when the prey moves 100 times faster than the predator ($\alpha = 100$), the predicted wavelength is about an order of magnitude larger (over 20) and the time period is closer to the limit cycle of the non-spatial model (87%). For the predator invasion scenario, varying α affects both wavelength and wave direction (upwards and downwards pointing triangles in Fig. 4(d) correspond to waves travelling to the left and right, respectively); note that in all of our landscape obstacle simulations (circles), the predicted waves travel to the right, away from the landscape obstacle. When $\alpha < 0.8$, invasions generate low wavelength waves, moving in the direction of the invasion front (downwards pointing triangles), whereas when $\alpha > 1$ invasions generate higher wavelength waves moving in the opposite direction to the invasion front (upwards pointing triangles). This illustrates two key points: that the ratio of the dispersal rates (α) can also affect the wave direction, and that in some regions of parameter space the wave properties can be very sensitive to changes in the ratio of the dispersal rates. For example changing α from 1 to 0.5 changes the waves generated by predator invasion from having a wavelength of about 7, moving away from the invasion front, to a wavelength of about 2 moving towards the invasion front (Fig. 4(d)).

4. Discussion

The key message from our results is that incorporating density-dependent dispersal does not dramatically affect the predicted spatiotemporal dynamics of our model cyclic populations: it has only a limited effect on both the shape of the wave family and the waves arising from two specific wave selection mechanisms.

In particular, the effects are generally much less than those arising from variation in the ratio of the diffusion coefficients. However, these conclusions do not imply that density-dependent dispersal will not have an important role on the spatiotemporal dynamics observed in biological systems. For example, if the observed wavelength is at the limit of what it is possible to detect in the field then density-dependent dispersal may be the difference between detection or not.

Readers with a particular system in mind should assess whether the magnitudes of the effects shown in our study would be significant for their own study system. First of all though, it is important to bear in mind that the results presented here only apply to the kinetic equations studied and the results may well be quite different for another system. However, taking as a specific example the cyclic larch budmoth–parasitoid interaction (Turchin, 2003), if this could be modelled using our predator–prey equations (with or without accounting for likely changes in plant quality; see Turchin, 2003) then we would expect the ratio of their dispersal rates to be especially important in the observed wave properties, and although we have no knowledge of density-dependence in the dispersal rates, we would expect density-dependence in the dispersal rates to be less important (Fig. 3(c, d)). In this example, one would have to be careful in interpreting a non-spatial model that predicted cycles of the same period as those observed in the field (9-yr cycles in this case, (Turchin, 2003)). This is because our results on wave families predict that in a spatial context, periods as low as 4 yr are possible. However, the difference between the spatial and non-spatial scenarios may be much less than this, depending on the ratio of the dispersal coefficients and on the wave selection mechanism. For example, if the dispersal rate of the larch budmoth was 100 times more than that of its parasitoid ($\alpha = 100$), and the waves were generated by a landscape obstacle, then the selected wave would have a time period closer to the limit cycle of the kinetics (Fig. 4(d)). Effects of differing dispersal rates on the spatiotemporal dynamics of larch budmoth populations were indeed found by Bjørnstad et al. (2002) and Johnson et al. (2006) in their spatial tri-trophic models of the larch budmoth, parasitoid, and habitat quality interactions. In particular, Johnson et al. (2006) found that the dispersal rates of the larch budmoth and their parasitoid influenced the dominant period of the population cycles. From their results, it is clear that both the ratio and the product of the dispersal rates affect the predicted time period (see their Fig. 2(b)). In reaction–diffusion models such the one we studied here, changing the product of the dispersal rates is simply equivalent to rescaling the spatial coordinate, resulting in no qualitative changes to the predicted dynamics. However, in the discrete space and time model studied by Johnson et al. (2006) this is no longer true, and they find an effect of changing both the ratio and the product of the dispersal rates. Our study highlights that different wave selection mechanisms can also influence how the dispersal rates affect the resulting wave properties (compare Fig. 2(b) in Johnson et al. (2006) with our Fig. 4(d), for example). It would therefore be informative to know whether there are plausible alternative wave selection mechanisms operating in the larch budmoth system, and whether modelling them would alter the predictions of the Johnson et al. (2006) model. As a general point for future modelling studies, it would be instructive for those modelling periodic travelling waves in cyclic populations to note how the time period in their simulations is affected by adding space to their models, as done here and by Johnson et al. (2006).

Many previous models of population dynamics have assumed discrete, rather than continuous, units for space or time. In the larch budmoth system discussed above, for example, the non-spatial dynamics are typically modelled using discrete time

equations (Turchin, 2003), and some studies have represented space using a coupled-map lattice (Bjørnstad et al., 2002; Johnson et al., 2004, 2006). Using such a modelling framework, Bjørnstad et al. (2002) found that different spatiotemporal behaviours emerged for different ratios and magnitudes of the larch budmoth dispersal rates when there was a gradient in habitat quality. It is therefore important to question the effects of the modelling framework used (discrete space and time versus continuous space and time) relative to the differences in the biological details. Would the results reported in our study differ significantly if we modelled space and time as discrete units? We do not know the answer but, based on previous comparisons of modelling frameworks (Sherratt et al., 1997), we predict that, whilst such changes would probably quantitatively affect our findings, our overall conclusions would remain unchanged. One advantage of discrete time is that it implicitly incorporates annual forcing. When interpreting time period predictions from continuous time models, it should be remembered that annual forcing will typically constrain time period to be a whole number of years; mathematically, the population cycles are entrained with the annual forcing. Explicit inclusion of such forcing is a natural area for future study (see preliminary work by Webb and Sherratt, 2004).

One omission from our results is how wave stability changes along the wave family. Unstable waves typically develop into irregular spatiotemporal oscillations, whereas stable waves persist over large domains and long times. We have performed a detailed stability analysis to determine how wave stability varies along the travelling wave families and this showed that the boundary between stable and unstable travelling waves (on infinite domain lengths) is affected by both the gradient of density-dependent dispersal (m) and the ratio of the diffusion coefficients (α). This analysis also confirmed that a few of the waves selected in our simulations are in fact unstable. However, in these simulations the instabilities only became apparent on very large domains, behind a large region (at least ten wavelengths) of apparently stable waves (see Fig. C.2 in Appendix C for an example). It seems unlikely that ecological systems exist with habitats that are sufficiently large and unbroken to allow the detection of wave break up after, say, 10 wavelengths have been generated (behind the invasion front or the landscape obstacle). Therefore, although the stability information is of mathematical interest, its ecological implications are limited. It is conceivable however that the effects of density-dependent dispersal on travelling wave stability may be more important if we had modelled different ecological interactions (host–parasite, vegetation–grazer) or used different parameters, and we provide the results of our stability analysis in Appendix C for information.

This study adds to the body of theoretical results on the potential consequences of density-dependent dispersal on population, and metapopulation, dynamics, and provides a theoretical underpinning for future studies investigating more realistic scenarios. Taken together, the findings from these studies and our own could support the exclusion of density-dependent dispersal from general modelling studies of population dynamics unless quantitative precision for specific systems is important. However, it is plausible that density-dependent dispersal, even in the way we have modelled it here, could still dramatically affect the model predictions for other sets of reaction kinetics. Our findings argue for conducting more studies into the importance of different dispersal properties on the spatiotemporal dynamics of populations, and argue strongly against using non-spatial models to predict the temporal dynamics of populations where there is evidence of periodic travelling waves in abundance.

Acknowledgements

M.J.S. was supported in part by a Natural Environment Research Council (NERC) Environmental Mathematics and Statistics Studentship (NER/S/A/2000/03198) and X.L. was supported by a NERC Grant (GR3/12956). We thank Gabriel Lord (Heriot-Watt), Simon Malham (Heriot-Watt), Jens Rademacher (CWI, Amsterdam) and Björn Sandstede (Surrey) for helpful advice and discussions.

Appendix A. Non-dimensionalization of the predator–prey model

The predator–prey model we use was introduced by Rosenzweig and MacArthur (1963) and is commonly used as a standard predator–prey model in theoretical ecology (Turchin, 2003). In fully dimensional form the spatial version of these equations can be written as

$$\frac{\partial N}{\partial T} = \frac{\partial}{\partial X} \left(D_N(N) \frac{\partial N}{\partial X} \right) + k_1 N \left(1 - \frac{N}{k_2} \right) - \frac{k_3 NP}{N + k_4}, \quad (\text{A.1a})$$

$$\frac{\partial P}{\partial T} = D_P \frac{\partial^2 P}{\partial X^2} + \frac{k_5 k_3 NP}{N + k_4} - k_6 P, \quad (\text{A.1b})$$

where N and P are the prey and predator population sizes (units: individuals), respectively, D_N and D_P are the prey and predator dispersal rates ($\text{km}^2 \text{yr}^{-1}$), respectively, k_1 is the maximum prey per-capita growth rate (yr^{-1}), k_2 is the prey carrying capacity (individuals), k_3 is the maximum per capita killing rate (yr^{-1}) of prey by predators, k_4 is the half-saturation constant in the rate of prey consumption by predators (individuals), k_5 is the conversion efficiency of prey eaten to predators (a proportion), and k_6 is the predator death rate (yr^{-1}). We then use the rescalings

$$N = uk_2, \quad T = t/k_1, \quad X = x\sqrt{D_0/k_1},$$

$$D_N(N) = D_u(u)D_0,$$

$$D_P = D_v D_0, \quad P = vk_1 k_2/k_3, \quad k_4 = \kappa k_2,$$

$$k_5 = \sigma k_1/k_3, \quad k_6 = \mu k_1.$$

These give the spatial predator–prey equations used in our study. For the dispersal rate scaling D_0 ($\text{km}^2 \text{yr}^{-1}$), $D_0 = \sqrt{D_P D_N(N_S)}$, where N_S is the value of N at the coexistence steady state; this implies $D_v = 1/D_u(u_s)$.

Appendix B. Numerical analysis of travelling wave families

We first re-write Eqs. (1a) and (1b) as

$$\frac{\partial u}{\partial t} = D_u(u) \frac{\partial^2 u}{\partial x^2} + \frac{\partial D_u(u)}{\partial u} \left(\frac{\partial u}{\partial x} \right)^2 + f(u, v), \quad (\text{B.1a})$$

$$\frac{\partial v}{\partial t} = D_v \frac{\partial^2 v}{\partial x^2} + g(u, v) \quad (\text{B.1b})$$

with the same definitions as in the main text. The standard way of analysing travelling wave solutions of Eqs. (B.1a) and (B.1b) is to replace space and time by one coordinate that moves along with the periodic travelling wave. Mathematically, the appropriate conversion is to use the travelling wave coordinate $z = (x/c) - t$, where c is the wave speed. This gives

$$(D_u(U)/c^2)U'' + D'_u(U)(U'/c)^2 + U' + f(U, V) = 0, \quad (\text{B.2a})$$

$$(D_v/c^2)V'' + V' + g(U, V) = 0, \quad (\text{B.2b})$$

where $U(z) = u(x, t)$, $V(z) = v(x, t)$, and prime denotes d/dz . This fourth-order system of ordinary differential equations predicts stationary wave forms in the co-moving frame. Eqs. (B.2a) and (B.2b) can then be written as a system of four first-order ordinary differential equations in the standard way

$$U' = A, \tag{B.3a}$$

$$A' = (-c^2/D_u(U))(A + D'_u(U)(A/c)^2 + f(U, V)), \tag{B.3b}$$

$$V' = B, \tag{B.3c}$$

$$B' = (-c^2/D_v)(B + g(U, V)). \tag{B.3d}$$

Steady-state solutions to this system are of the form $(U, A, V, B) = (u_s, 0, v_s, 0)$, with (u_s, v_s) being the spatially uniform steady-state solutions of Eqs. (B.1a) and (B.1b) that give rise to stable limit cycles through a Hopf bifurcation. Standard linear analysis of Eqs. (B.3a)–(B.3d) about these steady states reveals that the local stability of these steady states changes at a Hopf bifurcation wave speed c_{Hopf} . These steady-state solutions are generally stable for speeds below c_{Hopf} but unstable for speeds greater than c_{Hopf} . This Hopf bifurcation point corresponds to the origin of the travelling wave families and can be calculated analytically (we omit the calculation here for brevity).

Using the software package AUTO (Doedel et al., 1991a,b; Doedel, 1981) we can track the family of travelling wave solutions arising from c_{Hopf} in Eqs. (B.3a)–(B.3d) and study changes in the wave family shape caused by varying parameter values. AUTO is a software tool partly designed for continuation and bifurcation problems in ordinary differential equations. In this study, we use it for continuation. In other words, we use it to locate a periodic solution (a periodic travelling wave) to Eqs. (B.3a)–(B.3d), and then track how the properties of that periodic travelling wave vary as we gradually change the equation parameters. We first use AUTO to compute the eigenvalues for Eqs. (B.3a)–(B.3d), with a given set of reaction kinetics and $(U, A, V, B) = (u_s, 0, v_s, 0)$, for increasing c through c_{Hopf} . This allows AUTO to detect c_{Hopf} . We then use AUTO to continue along the wave family arising from c_{Hopf} , for increasing c . We also use AUTO to label solutions of given time periods along the family. We can then perform continuations from these labelled points to track how the properties of waves of a given time period vary with α or m . A detailed example of the use of AUTO for calculating travelling wave families for predator–prey reaction–diffusion equations accompanies a recent review of periodic travelling waves in cyclic populations by Sherratt and Smith (2008), and is available at <http://www.ma.hw.ac.uk/~jas/supplements/ptwreview/index.html>.

Appendix C. Analysis of travelling wave stability

We also used AUTO to calculate the stability of travelling wave solutions, for which the methodology is considerably more complicated. Our approach is identical to that used by Smith and Sherratt (2007) and is described in general terms by them and in much more detail by (Rademacher et al. (2007); see also Sandstede (2002)). The recent review of periodic travelling waves in cyclic populations by Sherratt and Smith (2008) also includes a detailed example of using AUTO to calculate wave stability for predator–prey reaction–diffusion equations (available at <http://www.ma.hw.ac.uk/~jas/supplements/ptwreview/index.html>). However we give a broad overview here.

We wish to study whether small perturbations to periodic travelling wave solutions of Eqs. (B.1a) and (B.1b) will grow or decay. If they decay then the wave is locally stable, and if they grow then the wave is unstable. Strictly, it is “essential stability”

that we are determining; other types of stability can be more relevant on finite domains (see Sandstede and Scheel, 2000). The standard approach to studying such stability is therefore to linearise Eqs. (B.2a) and (B.2b) about the periodic travelling wave solutions and then study their eigenvalues. However, rather than discrete eigenvalues, we are concerned with unbounded domains, for which there is an infinite spectrum of eigenvalues (Rademacher et al., 2007; Sandstede, 2002). Our intention is therefore to calculate this spectrum; if any eigenvalues have positive real part then we infer that the wave is (essentially) unstable. We consider perturbations of the form

$$u(z, t) = U(z) + e^{\lambda t} \bar{u}(z), \tag{C.1a}$$

$$v(z, t) = V(z) + e^{\lambda t} \bar{v}(z), \tag{C.1b}$$

where $|\bar{u}| \ll |U|$, $|\bar{v}| \ll |V|$, λ is an eigenvalue and t is time; recall that (U, V) is the periodic travelling wave solution. Substituting these solutions into Eqs. (B.1a) and (B.1b) and performing a Taylor expansion gives the eigenfunction equations

$$\lambda \bar{u} = D_u(U) \bar{u}'' + D'_u(U) [\bar{u} U'' + U' \bar{u}'] + D''_u(U) \bar{u}' (U')^2 + c \bar{u}' + \bar{u} f_u + \bar{v} f_v, \tag{C.2a}$$

$$\lambda \bar{v} = D_v \bar{v}'' + c \bar{v}' + \bar{u} g_u + \bar{v} g_v, \tag{C.2b}$$

with boundary conditions $\bar{u}(0) = \bar{u}(L)e^{i\gamma}$ and $\bar{v}(0) = \bar{v}(L)e^{i\gamma}$. Here the subscripts on f and g denote their first derivatives with respect to u or v , and L is the wavelength. Boundedness requires that perturbations do not grow or decay in magnitude over each wavelength. However, there is no constraint on the phase change of the perturbation over a wavelength. Thus the appropriate boundary conditions are $\bar{u}(0) = \bar{u}(L)e^{i\gamma}$ and $\bar{v}(0) = \bar{v}(L)e^{i\gamma}$, where γ can take any value between 0 and 2π (Sandstede, 2002). We need to obtain the eigenvalues for all possible phase shifts γ .

Stability analysis proceeds by first calculating eigenvalues corresponding to eigenfunctions that are periodic over one wavelength ($\gamma = 0$), by discretising in z to give a (large) algebraic eigenvalue problem; we consider only eigenvalues with an appropriately large real part. The spectrum is then computed in AUTO by continuation of the real and imaginary parts of these eigenvalues as γ is increased from 0 to 2π . The continuation must be done starting separately from each of the eigenvalues calculated for the $\gamma = 0$ case.

Using this technique we can identify critical points in the wave family (such as a critical wavelength) at which the wave stability changes. In all cases we studied, wave stability changes through an Eckhaus instability (Rademacher et al., 2007; Tuckerman and Barkley, 1990). This means that the dominant perturbation grows monotonically in time, rather than having the form of growing oscillations. Mathematically, this is convenient as it allows us to perform numerical continuations in the gradient of density-dependence (m) and the ratio of the diffusion coefficients (α) to see how the position of the stability boundary varies. Specifically, we differentiate Eqs. (C.2a) and (C.2b) twice with respect to γ . This gives a system of coupled differential equations that includes the second derivative of the real part of the eigenvalue, zeros of which define Eckhaus points. We numerically continue the locations of these zeros to trace the stability/instability boundary for periodic waves. Further details of this procedure are given in Rademacher et al. (2007).

Using these techniques, we found that both the gradient of density-dependence (m) and the ratio of the diffusion coefficients (α) influence the location of the stability boundary. We illustrate this in Fig. C.1, which is identical to Fig. 4 except that the stability information is also included. For the lambda-omega equations all waves picked out by zero-boundary conditions lie in the region of

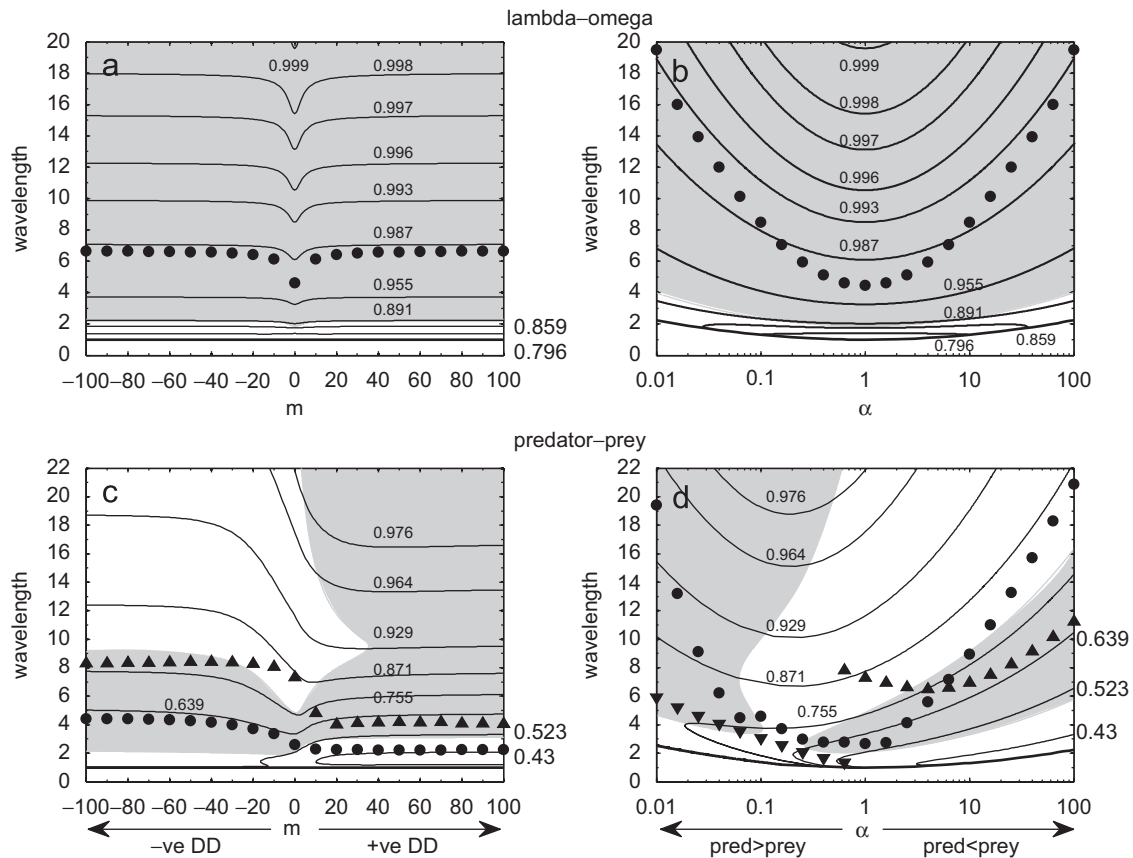


Fig. C.1. Comparison of the effects of varying the gradient of density-dependent dispersal m , between -100 (strong negative density-dependence) and 100 (strong positive density-dependence) with varying the ratio of constant diffusion coefficients $\alpha = D_u/D_v$ ($m = 0$) between 0.01 and 100 , on the wavelengths of periodic travelling waves (symbols) picked out by simulations of Eqs. (1a) and (1b). Note that α determines D_u and D_v , because our non-dimensionalization implies that $D_u D_v = 1$. The figure is exactly as in Fig. 4 of the main text except that here the results of the stability analysis are included, with stable waves lying within the grey shaded region and unstable waves lying within the white region above the thick black line. This line is the boundary of the region in which periodic travelling waves exist. Note that for the predator–prey equations some selected waves lie in the unstable region. In these cases, spatiotemporal irregularities develop behind a large region of waves, see for example Fig. C.2.

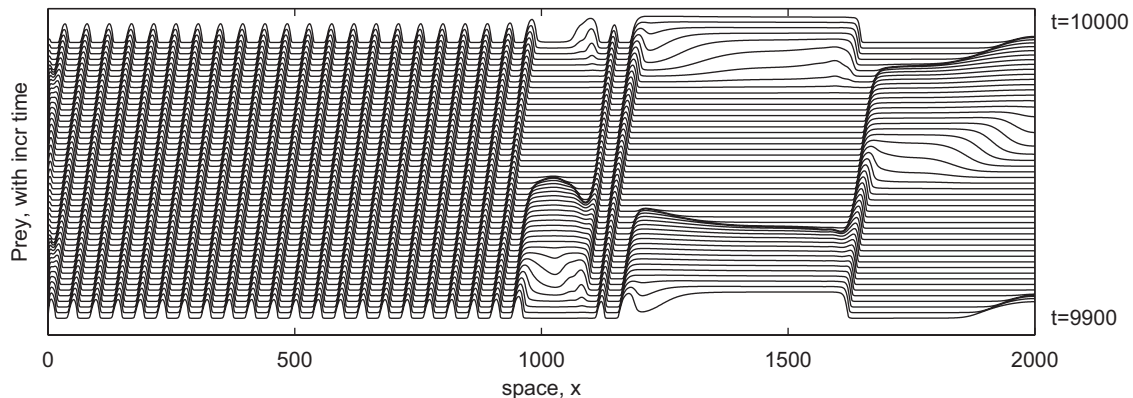


Fig. C.2. Unstable periodic travelling waves arising from a landscape obstacle (at $x = 0$) in a simulation of Eqs. (1a) and (1b) with predator–prey reaction kinetics (2). The boundary conditions are $(u, v) = (0, 0)$ at the left boundary (simulating the edge of an obstacle, or of an inhospitable habitat) and $du/dx = dv/dx = 0$ at the right boundary. This simulation started (at $t = 0$) with predator and prey densities chosen randomly from a uniform distribution between 0 and 1 . Parameter values are $\sigma = 0.15$, $\mu = 0.05$, and $\kappa = 0.2$, $D_{u,max} = 10^{0.5}$ and $D_{u,min} = 10^{-0.5}$ (implying $D_v = 1$). We also assume strong positive density-dependent dispersal, $m = 100$, corresponding to the right-most circle in Fig. C.1(c).

stable waves. However, for the predator–prey equations some selected waves are unstable. In Fig. C.2 we give one example of the spatiotemporal dynamics of an unstable case. Spatiotemporal irregularities develop behind a large region of what visually appears to be stable waves. This behaviour is typical of the unstable waves that occur in our simulations. As mentioned in the main text, it seems unlikely that ecological systems exist with

sufficiently large domains (habitats) to allow the detection of wave break up behind a large region of travelling waves. Therefore, although the stability information is of mathematical interest, its ecological implications are limited in these scenarios. However, the methods described here may be useful in models of other systems that predict unstable waves, which rapidly decay into spatiotemporal irregularities.

References

- Amarasekare, P., 1998. Interactions between local dynamics and dispersal: insights from single species models. *Theor. Popul. Biol.* 53, 44–59.
- Ashwin, P., Bartuccelli, M.V., Bridges, T.J., Gourley, S.A., 2002. Travelling fronts for the KPP equation with spatio-temporal delay. *Z. Angew. Math. Phys.* 53, 103–122.
- Auchmuty, J.F.G., Nicolis, G., 1976. Bifurcation analysis of reaction–diffusion equations 3. Chemical oscillations. *Bull. Math. Biol.* 38, 325–350.
- Baltensweiler, W., Benz, G., Bovey, P., Delucchi, V., 1977. Dynamics of Larch bud moth populations. *Annu. Rev. Entomol.* 22, 79–100.
- Berryman, A., 2002. Population cycles: causes and analysis. In: Berryman, A. (Ed.), *Population Cycles: The Case for Trophic Interactions*, vol. 1. Oxford University Press, Oxford, pp. 3–28.
- Best, A.S., Johs, K., Munkemuller, T., Travis, J.M.J., 2007. Which species will successfully track climate change? The influence of intraspecific competition and density dependent dispersal on range shifting dynamics. *Oikos* 116, 1531–1539.
- Bjørnstad, O.N., Peltonen, M., Liebhold, A.M., Baltensweiler, W., 2002. Waves of Larch budmoth outbreaks in the European Alps. *Science* 298, 1020–1023.
- Bowler, D.E., Benton, T.G., 2005. Causes and consequences of animal dispersal strategies: relating individual behaviour to spatial dynamics. *Biol. Rev.* 80, 205–225.
- Brandt, M.J., Lambin, X., 2007. Movement patterns of a specialist predator, the weasel *Mustela nivalis* exploiting asynchronous cyclic field vole *Microtus agrestis* populations. *Acta Theriol.* 52, 13–25.
- Cantrell, R.S., Cosner, C., Fagan, W.F., 1998. Competitive reversals inside ecological reserves: the role of external habitat degradation. *J. Math. Biol.* 37, 491–533.
- Codling, E.A., Plank, M.J., Benhamou, S., 2008. Random walk models in biology (review). *J. R. Soc. Interface* 5, 813–834.
- Denno, R.F., Peterson, M.A., 1995. Density dependent dispersal and its consequences for population dynamics. In: Cappuccino, N., Price, P.W. (Eds.), *Population Dynamics: New Approaches and Synthesis*. Academic Press, New York, pp. 113–130.
- Doedel, E., Keller, H.B., Kernevez, J.P., 1991a. Numerical analysis and control of bifurcation problems (I): bifurcation in finite dimensions. *Int. J. Bifurcat. Chaos* 1, 493–520.
- Doedel, E., Keller, H.B., Kernevez, J.P., 1991b. Numerical analysis and control of bifurcation problems (II): bifurcation on infinite dimensions. *Int. J. Bifurcat. Chaos* 1, 723–745.
- Doedel, E.J., 1981. AUTO: a program for the automatic bifurcation analysis of autonomous systems. *Congr. Numer.* 30, 265–284.
- Drover, J.D., Ermentrout, B., 2003. Nonlinear coupling near a degenerate Hopf (Bautin) bifurcation. *SIAM J. Appl. Math.* 63, 1627–1647.
- Ermentrout, B., Chen, X.F., Chen, Z.X., 1997. Transition fronts and localized structures in bistable reaction–diffusion equations. *Physica D* 108, 147–167.
- Garvie, M.R., 2007. Finite-difference schemes for reaction–diffusion equations modeling predator–prey interactions in MATLAB. *Bull. Math. Biol.* 69, 931–956.
- Giraudoux, P., Delattre, P., Habert, M., Quere, J.P., Deblay, S., Defaut, R., Duhamel, R., Moissenet, M.F., Salvi, D., Truchetet, D., 1997. Population dynamics of fossorial water vole (*Arvicola terrestris* scherman): a land use and landscape perspective. *Agric. Ecosyst. Environ.* 66, 47–60.
- Hagan, P.S., 1982. Spiral waves in reaction–diffusion equations. *SIAM J. Appl. Math.* 42, 762–786.
- Hauzy, C., Hulot, F.D., Gins, A., Loreau, M., 2007. Intra- and interspecific density dependent dispersal in an aquatic prey–predator system. *J. Anim. Ecol.* 76, 552–558.
- Huu, T.N., Auger, P., Lett, C., Marva, M., 2008. Emergence of global behaviour in a host–parasitoid model with density dependent dispersal in a chain of patches. *Ecol. Complexity* 5, 9–21.
- Ims, R.A., Andreassen, H.P., 2005. Density dependent dispersal and spatial population dynamics. *Proc. R. Soc. B—Biol. Sci.* 272, 913–918.
- Ims, R.A., Hjermann, D.O., 2001. Condition-dependent dispersal. In: Clobert, J., et al. (Eds.), *Dispersal*. Oxford University Press, Oxford, pp. 203–216.
- Johnson, D.M., Bjørnstad, O.N., Liebhold, A.M., 2004. Landscape geometry and travelling waves in the Larch budmoth. *Ecol. Lett.* 7, 967–974.
- Johnson, D.M., Bjørnstad, O.N., Liebhold, A.M., 2006. Landscape mosaic induces traveling waves of insect outbreaks. *Oecologia* 148, 51–60.
- Johst, K., Brandl, R., 1997. The effect of dispersal on local population dynamics. *Ecol. Modelling* 104, 87–101.
- Kopell, N., Howard, L.N., 1973. Plane-wave solutions to reaction–diffusion equations. *Stud. Appl. Math.* 52, 291–328.
- Kuussaari, M., Nieminen, M., Hanski, I., 1996. An experimental study of migration in the Glanville fritillary butterfly *Melitaea cinxia*. *J. Anim. Ecol.* 65, 791–801.
- Lambin, X., Elston, D.A., Petty, S.J., MacKinnon, J.L., 1998. Spatial asynchrony and periodic travelling waves in cyclic populations of field voles. *Proc. R. Soc. London Ser. B—Biol. Sci.* 265, 1491–1496.
- Lambin, X., Aars, J., Pieltney, S.B., 2001. Dispersal, intraspecific competition, kin competition and kin facilitation: a review of the empirical evidence. In: Clobert, J., et al. (Eds.), *Dispersal*. Oxford University Press, Oxford, pp. 110–122.
- Lutscher, F., 2008. Density dependent dispersal in integrodifference equations. *J. Math. Biol.* 56, 499–524.
- MacKinnon, J.L., Petty, S.J., Elston, D.A., Thomas, C.J., Sherratt, T.N., Lambin, X., 2001. Scale invariant spatio-temporal patterns of field vole density. *J. Anim. Ecol.* 70, 101–111.
- Massey, F.P., Smith, M.J., Lambin, X., Hartley, S.E., 2008. Are silica defences in grasses driving vole population cycles? *Biol. Lett.* 13, 1234. Published online 15/05/08, doi:10.1098/rsbl.2008.0106.
- Matthysen, E., 2005. Density dependent dispersal in birds and mammals. *Ecography* 28, 403–416.
- Moss, R., Elston, D.A., Watson, A., 2000. Spatial asynchrony and demographic travelling waves during red grouse population cycles. *Ecology* 81, 981–989.
- Murray, J.D., 2003. *Multi-Species Waves and Practical Applications*, *Mathematical Biology II: Spatial Models and Biomedical Applications*, vol. II. Springer, Berlin, pp. 1–67.
- Murray, J.D., Stanley, E.A., Brown, D.L., 1986. On the spread of rabies among foxes. *Proc. R. Soc. B—Biol. Sci.* 229, 111–150.
- Pearce, I.G., Chaplain, M.A.J., Schofield, P.G., Anderson, A.R.A., Hubbard, S.F., 2006. Modelling the spatio-temporal dynamics of multi-species host–parasitoid interactions: heterogeneous patterns and ecological implications. *J. Theor. Biol.* 241, 876–886.
- Peltonen, M., Liebhold, A.M., Bjørnstad, O.N., Williams, D.W., 2002. Spatial synchrony in forest insect outbreaks: roles of regional stochasticity and dispersal. *Ecology* 83, 3120–3129.
- Petrovskii, S.V., Malchow, H., 1999. A minimal model of pattern formation in a prey–predator system. *Math. Comput. Modelling* 29, 49–63.
- Rademacher, J.D.M., Sandstede, B., Scheel, A., 2007. Computing absolute and essential spectra using continuation. *Physica D* 229, 166–183.
- Ranta, E., Kaitala, V., 1997. Travelling waves in vole population dynamics. *Nature* 390, 456.
- Rosenzweig, M.L., MacArthur, R.H., 1963. Graphical representation and stability conditions of predator–prey interaction. *Am. Nat.* 97, 209–223.
- Rouquette, J.R., Thompson, D.J., 2007. Patterns of movement and dispersal in an endangered damselfly and the consequences for its management. *J. Appl. Ecol.* 44, 692–701.
- Royama, T., MacKinnon, W.E., Kettela, E.G., Carter, N.E., Hartling, L.K., 2005. Analysis of spruce budworm outbreak cycles in New Brunswick, Canada, since 1952. *Ecology* 86, 1212–1224.
- Russell, C.A., Smith, D.L., Childs, J.E., Real, L.A., 2005. Predictive spatial dynamics and strategic planning for racoon rabies emergence in Ohio. *Plos Biol.* 3, 382–388.
- Saether, B.-E., Engen, S., Lande, R., 1999. Finite metapopulation models with density dependent migration and stochastic local dynamics. *Proc. R. Soc. B—Biol. Sci.* 266, 113–118.
- Sandstede, B., 2002. Stability of travelling waves. In: Fiedler, B. (Ed.), *Handbook of Dynamical Systems II*. North-Holland, Amsterdam, pp. 983–1055.
- Sandstede, B., Scheel, A., 2000. Absolute and convective instabilities of waves on unbounded and large bounded domains. *Physica D* 145, 233–277.
- Schwartz, M.K., Mills, L.S., McKelvey, K.S., Ruggiero, L.F., Allendorf, F.W., 2002. DNA reveals high dispersal synchronizing the population dynamics of *Canada lynx*. *Nature* 415, 520–522.
- Sherratt, J.A., 1994. On the evolution of periodic plane-waves in reaction–diffusion systems of lambda-bd-omega type. *SIAM J. Appl. Math.* 54, 1374–1385.
- Sherratt, J.A., 2001. Periodic travelling waves in cyclic predator–prey systems. *Ecol. Lett.* 4, 30–37.
- Sherratt, J.A., 2003. Periodic travelling wave selection by Dirichlet boundary conditions in oscillatory reaction–diffusion systems. *SIAM J. Appl. Math.* 63, 1520–1538.
- Sherratt, J.A., Smith, M.J., 2008. Periodic travelling waves in cyclic populations: field studies and reaction–diffusion models. *J. R. Soc. Interface* 5, 483–505.
- Sherratt, J.A., Eagan, B.T., Lewis, M.A., 1997. Oscillations and chaos behind predator–prey invasion: mathematical artefact or ecological reality. *Philos. Trans. R. Soc. B—Biol. Sci.* 352, 21–38.
- Sherratt, J.A., Lambin, X., Sherratt, T.N., 2003. The effects of the size and shape of landscape features on the formation of traveling waves in cyclic populations. *Am. Nat.* 162, 503–513.
- Smith, J.E., Batzli, G.O., 2006. Dispersal and mortality of prairie voles (*Microtus ochrogaster*) in fragmented landscapes: a field experiment. *Oikos* 112, 209–217.
- Smith, M.J., Sherratt, J.A., 2007. The effects of unequal diffusion coefficients on periodic travelling waves in oscillatory reaction–diffusion systems. *Physica D* 236, 90–103.
- Sutherland, W.J., Gill, J.A., Norriss, K., 2002. Density dependent dispersal in animals: concepts, evidence, mechanisms and consequences. In: Bullock, J.M., et al. (Eds.), *Dispersal Ecology*. Blackwell, Oxford, pp. 113–133.
- Tenow, O., Nilssen, A.C., Bylund, H., Hogstad, O., 2007. Waves and synchrony in *Epirrita autumnata*/*Operophtera brumata* outbreaks. I. Lagged synchrony: regionally, locally and among species. *J. Anim. Ecol.* 76, 258–268.
- Tuckerman, L.S., Barkley, D., 1990. Bifurcation-analysis of the Eckhaus instability. *Physica D* 46, 57–86.
- Turchin, P., 2003. *Complex Population Dynamics: A Theoretical/Empirical Synthesis*. Princeton University Press, Princeton.
- Webb, S.D., Sherratt, J.A., 2004. Oscillatory reaction–diffusion equations with temporally varying parameters. *Math. Comp. Modelling* 39, 45–60.
- Ydenberg, R., 1987. Nomadic predators and geographical synchrony in microtine population cycles. *Oikos* 50, 270–272.
- Ylikarjula, J., Alaja, S., Laakso, J., Tesar, D., 2000. Effects of patch number and dispersal patterns on population dynamics and synchrony. *J. Theor. Biol.* 207, 377–387.